Supporting Information for

ORIGINAL ARTICLE

TPGS/hyaluronic acid dual-functionalized PLGA nanoparticles delivered through dissolving microneedles for markedly improved chemo-photothermal combined therapy of superficial tumor

Tingting Peng[a], Yao Huang[b], Xiaoqian Feng[b], Chune Zhu[c], Shi Yin[b], Xinyi Wang[d], Xuequn Bai[b], Xin Pan[b,*], Chuanbin Wu[a,b,*]

[a]*College of Pharmacy, Jinan University, Guangzhou 510632, China*

[b]*School of Pharmaceutical Sciences, Sun Yat-sen University, Guangzhou 510006, China*

[c]*School of Traditional Chinese Medicine, Guangdong Pharmaceutical University, Guangzhou 510006, China*

[d]*Guanghua School of Stomatology, Hospital of Stomatology, Sun Yat-sen University, Guangzhou 510055, China*

[*]Corresponding authors. Tel.: +862039943120; fax: +862039943117 (Chuanbin Wu); Tel.: +86 2039943427; fax: +86 2039943115 (Xin Pan).

E-mail addresses: panxin2@mail.sysu.edu.cn (Xin Pan), wuchuanb@mail.sysu.edu.cn (Chuanbin Wu).

Running title: Dissolving microneedles encapsulating functionalized PLGA nanoparticles for strengthened anti-tumor effect

Supporting methods

1. Optimization of preparing TPGS functionalized PLGA nanoparticles

A nanoprecipitation method was used to prepare TPGS functionalized PLGA nanoparticles (NPs). Initially, the organic and aqueous solutions were prepared as follows: (1) PLGA, DOTAP and PTX were dissolved in acetone, (2) TPGS was

dissolved in the 4% (*w*/*w*) ethanol aqueous solution and heated to 65 ℃, and (3) ICG dissolved in 20% (*w*/*v*) methanol was mixed with organic or aqueous solution prior to preparation. Then, the organic phase was slowly added to the aqueous phase under constant magnetic stirring for 20 min at 35 ℃ to generate TPGS functionalized PLGA NPs. The obtained NPs were subjected to determining particle size, zeta potential and drug encapsulation efficiency (EE%).

The particle size, polydispersity index (PDI) and zeta potential of NPs were measured using Malvern Zetasizer Nano ZS90 (Malvern Instruments, Malvern, UK). The drug EE% was determined by ultracentrifugation. In detail, the fresh NPs were centrifuged at 35,000 rpm for 30 min by Optima L-100XP Ultracentrifuge (Beckman, USA) to isolate the NPs and free drug. The supernatant was collected to measure the free PTX or ICG content. The concentration of PTX was analyzed by HPLC according to the following condition: wavelength, 228 nm; mobile phase, acetonitrile and water (53/47, *v*/*v*); flow rate, 1.0 mL/min; column temperature, 37 ℃; injection volume, 20 μL. The concentration of ICG was measured by UV/Vis spectrometer (UV-2600, Shimadzu Co., Ltd., Japan) at 787 nm. The EE% was calculated as the following Eq. (1):

$$\text{EE}\ (\%) = \left(1 - \frac{\text{Free drug amount}}{\text{Total drug amount}}\right) \times 100 \qquad (1)$$

1.1. Influence of TPGS concentration on the physicochemical properties of NPs

Different concentrations of TPGS (1.0, 1.5 and 2.0 mg/mL) were used to prepare TPGS functionalized PLGA NPs and study their influence on the physicochemical properties of NPs. The organic phase consisted of PLGA (4.0 mg/mL) and PTX (0.2 mg/mL). 100 μl of ICG (1 mg/mL) was blended with 500 μL of PLGA acetone solution, followed by dropwise dripping into the TPGS aqueous solution to generate NPs. As shown in Fig. S1, TPGS concentration exerted almost no different effect on the particle size, surface charge and EE% of PTX, while the EE% of ICG increased with the growing TPGS concentration. Therefore, TPGS at the concentration of 2.0 mg/mL was selected for further study.

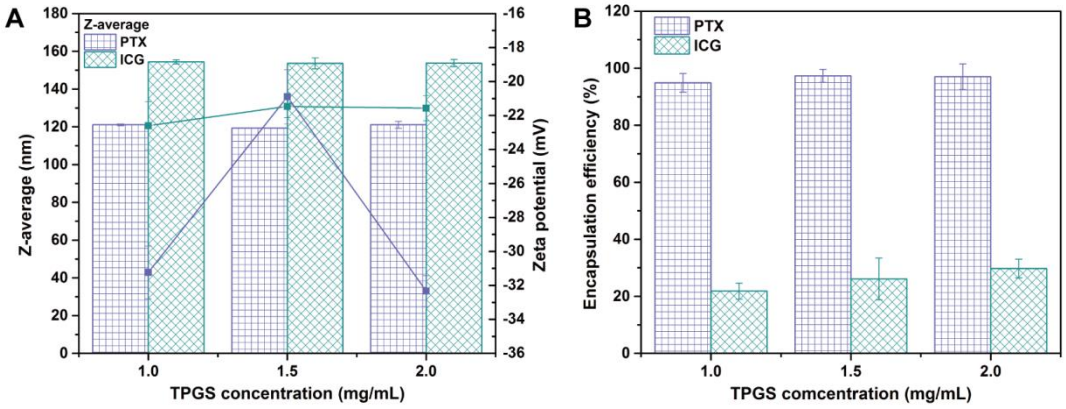

Figure S1 The influence of TPGS concentration on the physicochemical properties of TPGS functionalized PLGA NPs (Data are presented as mean or mean±SD, *n*=3): (A) the particle size and zeta potential of NPs, and (B) the EE% of ICG and PTX.

1.2. Influence of DOTAP amount on the physicochemical properties of NPs

As shown in Table S1, the preparation of TPGS functionalized PLGA NPs followed the same procedures described in Supporting Section 1.1, except that PLGA was partially substituted with DOTAP to improve the EE% of ICG. From Fig. S2, it could be seen that the addition of DOTAP at the polymer weight ratio of 10% and 20%, significantly enhanced the EE% of ICG. The probable reason was that the transition in the surface charge of NPs led to the increased absorption of ICG by electrostatic interaction force.

Table S1 Formulation compositions of TPGS functionalized PLGA nanoparticles containing different amount of DOTAP.

Formulation	Water phase	Oil phase				
	TPGS (mg/mL)	ICG (mg/mL)	PLGA (mg/mL)	DOTAP (mg/mL)	DOTAP amount (*w*/*w*)	PTX (mg/mL)
F0	2.0	1.0	4.0	0	0	0.2
F1			3.6	0.4	10%	
F2			3.2	0.8	20%	
F3			2.8	1.2	30%	

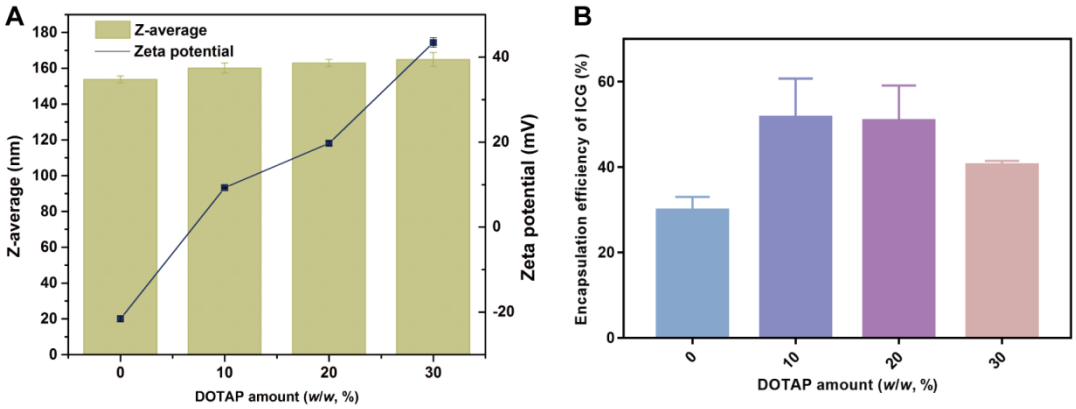

Figure S2 The influence of DOTAP amount on the physicochemical properties of TPGS functionalized PLGA NPs (Data are presented as mean or mean±SD, *n*=3).(A) the particle size and zeta potential of NPs, and (B) the EE% of ICG.

1.3. Influence of ICG mixing solution form on the physicochemical properties of NPs

Based on previous reports, there were two forms of mixing ICG solution during NPs preparation, one was to mix with the aqueous solution[1], and another one was to blend with the organic solution[2-4]. Herein, the influence of ICG mixing form on the physicochemical properties of NPs was investigated. The formulation (F2, shown in Table S1) was taken as an example.

The mixing form of ICG for NP preparation may alter the distribution of ICG in the NPs and further its physicochemical properties, since ICG is an amphiphilic and negatively charged compound[2]. As displayed in Table S2, mixing ICG solution with TPGS aqueous solution produced smaller and more uniform particle size, as well as a slightly higher zeta potential and EE% than mixing with organic solution. Accordingly, the mixture of ICG and TPGS was utilized to prepare TPGS functionalized NPs in the further study owing to the potential benefit of smaller particle size and higher EE%.

Table S2 The mixture form of ICG solution on the physicochemical properties of TPGS functionalized PLGA NPs. .

Mixture form of ICG solution	*Z*-average (nm)	PDI	Zeta potential (mV)	EE% of ICG (%)
Oil phase	162.83 ± 1.99	0.15 ± 0.02	19.73 ± 0.55	50.72 ± 8.41
Water phase	141.10 ± 1.26	0.13 ± 0.01	23.50 ± 3.08	52.30 ± 2.93

Data are presented as mean or mean ± SD (n=3).

2. Optimization of preparing TPGS/HA functionalized PLGA NPs

TPGS/HA functionalized NPs was prepared through the electrostatic crosslinking between positively charged TPGS functionalized NPs and negatively charged HA. Specifically, HA solution (1.0 mg/mL) was used to coat fresh TPGS functionalized NPs at the volume ratio of 1:3, 1:2, 2:3 and 5:6, under constant stirring for 10 min. As shown in Fig. S3, the zeta potential of NPs was shifted from positive charge (23.5 mV) to negative charge (about –23 mV) regardless of titration volume ratio, while the increase in particle size of NPs was about 20 nm and reached to a plateau only when the volume ratio of HA and TPGS functionalized NPs was ≥ 2:3. Therefore, 2:3 (*v*/*v*) of HA and TPGS functionalized NPs was selected to prepare TPGS/HA dual-functionalized PLGA NPs in the following study.

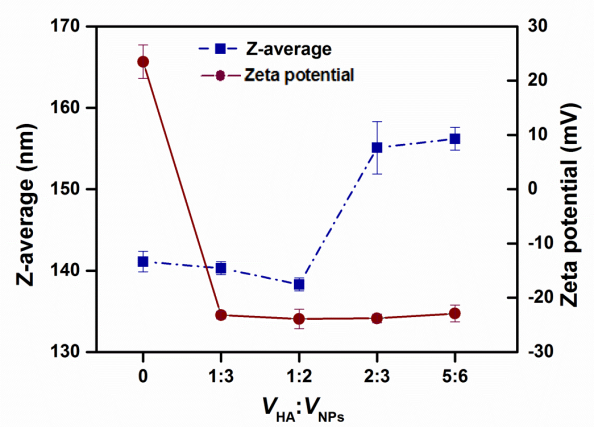

Figure S3 The influence of the titration volume ratio of HA solution to fresh TPGS functionalized PLGA NPs on the particle size and zeta potential (Data are presented

as mean or mean ±SD, *n*=3).

To sum up, the optimized formulation compositions (Table S3) was used to prepare the TPGS functionalized PLGA NPs. D10 NPs and D20 NPs showed approachable particle size (about 140 nm) and drug EE% (The EE% of PTX and ICG was about 90% and 50%, respectively.). However, D10 NPs showed higher cytotoxicity than D20 NPs (Fig. S4). Thereby, fresh D10 NPs was selected and coated by HA at the volume ratio of 3:2 for further study.

Table S3 The formulation compositions of TPGS functionalized PLGA nanoparticles.

Formulation	Water phase		Oil phase		
	TPGS (mg/mL)	ICG (mg/mL)	PLGA (mg/mL)	DOTAP (mg/mL)	PTX (mg/mL)
D10 NPs	2.0	1.0	3.6	0.4	0.2
D20 NPs			3.2	0.8	

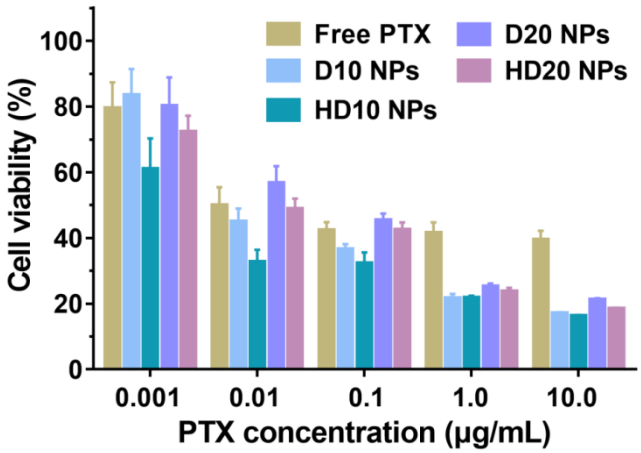

Figure S4 The 48 h cell viability of MDA-MB-231 cells incubated with free PTX,D10 NPs, HD10 NPs, D20 NPs and HD20 NPs at different PTX concentration (Data are presented as mean or mean ±SD, *n*=5).

3. Characterization of D10 NPs and HD10NPs

3.1. Particle size, zeta potential and encapsulation efficiency

The particle size, zeta potential and EE (%) of D10 NPs and HD10 NPs was determined as the protocol described in Supporting Section 1.

3.2. Morphology

D10 NPs, HD10 NPs and the NPs irradiated with a NIR laser (808 nm, 1 W/cm^2) for 5 min were stained by 3% phosphotungstic acid, and their morphologies were observed by a transmission electron microscope (TEM, JEOL, Tokyo, Japan) at an acceleration voltage of 120 kV.

3.3. Spectroscopic properties

The absorption spectra of free ICG solution, D10 NPs and HD10 NPs were scanned between 650–900 nm with UV/Vis spectrometer (UV-2600, Shimadzu Co., Ltd., Japan). Fluorescent spectra of ICG solution and ICG loaded NPs were recorded between 780–900 nm with excitation at 763 nm using fluorescent spectrometer (Fluoromax-4, HORIBA, USA).

3.4. In vitro photothermal conversion efficiency

2 mL of PBS solution, free ICG/D10 NPs/HD10 NPs solution loading 20 μg/mL of ICG were added to the 24-well plate, and separately illuminated by a laser (808 nm, 1 W/cm^2) for 5 min. The change in temperature of solution was monitored by an infrared thermal imaging camera (TiS75, Fluke, USA).

3.5. Fluorescent intensity

To assess the fluorescent stability of free ICG solution and ICG-loaded NPs, the aqueous solutions were stored at 37 ℃ for 7 days. The fluorescent intensity of solution was determined by fluorescent spectroscopy with excitation and emission wavelength at 763 and 820 nm, respectively. The concentration of ICG was 300 μg/mL, and the fluorescent intensity was measured at Days 0, 1, 3, 5 and 7. The relative fluorescent intensity was calculated as the percentage of initial fluorescent intensity.

3.6. In vitro release study

The release behavior of D10 NPs, HD10 NPs and HD10 NPs triggered by NIR LS was detected using a dialysis method. The NPs containing 200 μg PTX were added to the dialysis bags (MW cutoff 3500 Da), which was then placed in a 50 mL EP tube with 30 mL buffer solution (7:3 of pH 7.4 PBS and ethanol, *v*/*v*). The dialysis bags were stirred at 100 rpm/37 ℃ using an air bath shaking table (THZ-82BA, Jintan, China). Samples (2 mL each) were withdrawn at predetermined time intervals, and replaced by equivalent buffer solution. For the LS group, HD10 NPs were irradiated with a laser (808 nm, 1 W/cm^2) for 5 min. The samples were analyzed by HPLC to determine the cumulative release of PTX.

4. Cellular study

4.1. Cell culture

MDA-MB-231 cells were gifted from the lab of Prof. Ming Huang in Sun Yat-sen University. The cells were cultured in DMEM medium, supplemented with 10% fetal bovine serum in an incubator under 5% CO_2 at 37 ℃.

4.2. Cytotoxicity

MDA-MB-231 cells were seeded in 96-well plates at a density of 5×10^3 cells per well and cultured for 24 h. The previous medium was removed and replaced by the fresh medium containing free PTX, D10 NPs or HD10 NPs at various PTX concentration to co-incubate with cells for 24 or 48 h. To assess the anti-cancer effect of the chemo-photothermal combined therapy, the cells were further exposed to a near-infrared (NIR) laser (808 nm, 1 W/cm^2) for 5 min after 4 h of incubation, and cultured for another 20 h. The cells without any treatment were used as the negative control. After incubation, a mixed solution of CCK8 (10 μL) and fresh culture medium 90 μL) was added to each well to replace the previous medium and co-incubated with cells for another 2 h at 37 ℃ and 5% CO_2. Finally, the absorbance was measured at 450 nm by a micro plate reader (Epoch 2, Bio-Tek, USA).

4.3. Cell apoptosis

Annexin V-FITC/PI apoptosis kit was used to assess the apoptosis-inducing capability of different treatments. Specifically, the MDA-MB-231 cells were seeded in 6-well plates at a density of 2×10^5 cells per well and cultured for 24 h. Then, the cells treated with chemotherapy (free PTX/ICG, D10 and HD10 NPs) were incubated for 24 h, while the cells receiving chemo-photothermal combined therapy were simultaneously illuminated with a NIR laser (808 nm, 1 W/cm^2) for 5 min after 4 h of incubation. The concentration of PTX and ICG was 10 and 13 μg/mL, respectively. The attached and detached cells were collected, washed with cold PBS twice and suspended in the buffer solution. The suspended cells were double stained with 10 μL of PI and 5 μL of Annexin V-FITC, respectively, and were analyzed by the flow cytometry (EPICS XL, Beckman Coulter, USA).

4.4. Intracellular localization

To detect the mitochondrial localization of NPs, cells were seeded in 24-well glassy plate (Corning) at a density of 1×10^5 cells per well for 24 h. To avoid the interference of ICG fluoresence on mitochondria localization, D10 NPs or HD10 NPs loading sole cocumarin-6 were prepared as the procedures mentioned in Supporting Section 2.1, except that PTX was replaced by cocumarin-6. Cocumarin at the concentration of 10 μg/mL was used. The cells were incubated with free cocumarin-6, D10 NPs and HD10 NPs for 4 h. After incubation, the medium was removed and the cells were washed with cold PBS thrice. Then, the cells were immobilized with 4% (*v*/*v*) formaldehyde at 4 ℃ for 20 min, and incubated with MitoTracker Deep Red (500 nmol/L) at 37 ℃ for 1 h to labele mitochondria. Finally, the cells were washed using cold PBS and stained with DAPI to label nuclei for 15 min at room temperature. The treated cells were observed using confocal laser scanning microscope (CLSM, FV3000, Olympus, Japan). The excitation wavelength of DAPI, cocumarin-6 and MitoTracker Deep Red was set at 405, 488 and 644 nm, respectively.

The lysosome localization of NPs was detected and labeled using LysoTracker

DND 99 (500 nmol/L) as the procedures of mitochondrial localization. The treated cells were visualized by CLSM at the excitation wavelength of 405 nm (DAPI), 488 nm (cocumarin-6) and 577 nm (MitoTracker Deep Red).

As displayed in Fig. S5, the fluorescent signal of free coumarin-6 highly overlapped with that of Lyso Tracker, but only a slighty or no overlap in fluoresent signal was found in the D10 NPs and HD10 NPs. It was indicated that free coumarin-6 was mainly localized in the lysosome, while encapsulation of coumarin-6 into TPGS functionalized NPs could help to lysosome escape.

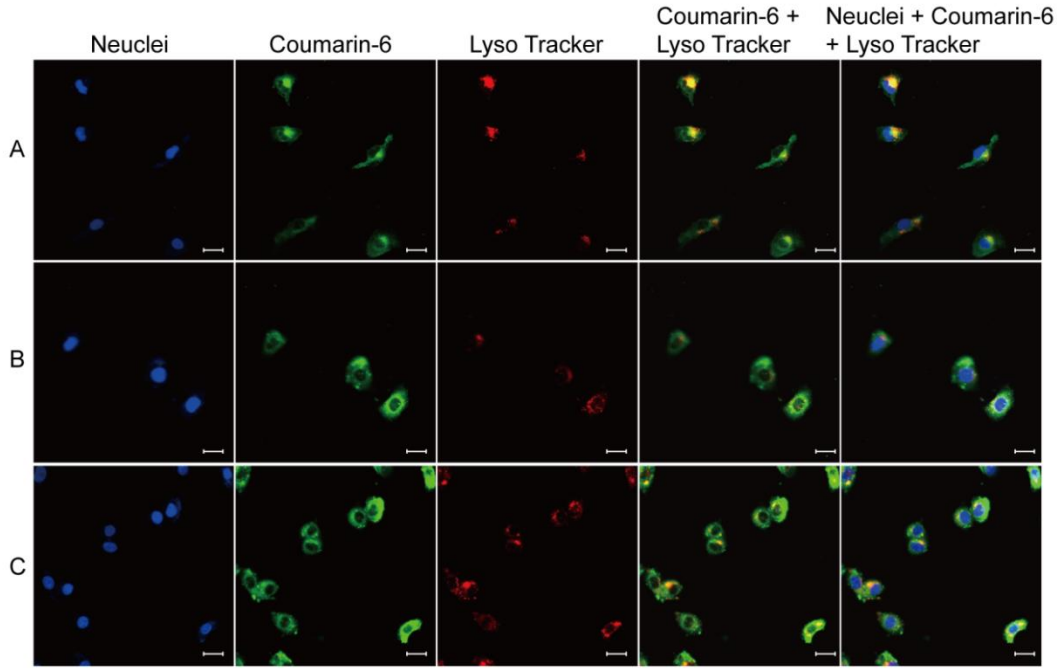

Figure S5 The distribution of coumarin-6 in the nucleus and lysosome of MDA-MB-231 cells after treatment with various formulations: (A) free coumarin-6, (B) D10 NPs, and (C) HD10 NPs. The scale bar=30 μm.

4.5. Caspase 9 and caspase 3 activity

The activation of caspase was determined using the chromogenic reaction between specific protease and peptide substrates. To evaluate the activity of caspase 9 and caspase 3, the MDA-MB-231 cells were seeded in 6-well plates at a density of 2×10^5 cells per well and cultured for 24 h. Then, the cells were exposed to complete culture medium (as a control) and different formulations (free PTX/ICG, D10 NPs and HD10

NPs) for 12 h. The concentration of PTX was 2.5 μg/mL. The cells treated with HD10 NPs were additionally irradiated with a NIR laser (808 nm, 1 W/cm^2) for 5 min after 4 h of incubation. After culture, the cells were harvested, lysed, and centrifuged based on the instructions of assay kit. The total protein content of each sample was measured by Bradford protein assay kit to normalize the obtained values. Finally, the absorbance of each sample was determined at 405 nm using a micro plate reader (Epoch 2, Bio-Tek, USA). The activity was calculated as the ratio of treatment group to the control group.

4.6. Western blotting

MDA-MB-231 cells were cultured in a dish (6 cm in diameter) and incubated for 8 h with complete culture medium HD10 and HD10 NPs with laser (808 nm, 1 W/cm^2, 5 min) treatment. Then, total protein was harvested and the proteins related to the tumor prognosis (survivin) and tumor metastasis (MMP-9 and α-tubulin) were analyzed by Western blotting. NADPH was used as the internal control.

5. Preparation and characterization of DMNs

5.1. Preparation of DMNs

A centrifugation method was used to prepare DMNs. The detailed steps were as follows: (1) 100 μl of 4:1 *v*/*v* of the NPs-PVA/PVP mixtures (the final concentration of PVA and PVP was 32 and 48 mg/mL, respectively.) were pipped into the micro-holes of DMNs, and centrifuged for 10 min at 4 ℃/4000 rpm to deposit the NPs into the tip. (2) The remaining solution was collected into the EP tube, and the DMNs continued to centrifuge at 4000 rpm for 30 min to allow the NPs to be sufficiently compressed at the tip of the needle and the water to be evaporated. (3) 80 μL of the collected nanosuspensions were again added to each patch of DMNs, and processed as the first two steps. (4) 150 μl of PVA (150 mg/mL)/PVP (250 mg/mL) mixed solution was added to the mold of DMNs, and then the DMNs mold was vacuum degassed for 10 min and centrifuged at 4000 rpm for 5 min. (5) The residual solution was scraped off the mold, followed by filling 250 μL of PVP solution into the

mold and centrifuging at 4000 rpm for 5 min to prepare the backing layer of DMNs. (6) The DMNs mold was placed in a desiccator to dry at room temperature for 36 h. The DMNs patched were gently peeled from the mold with a tweezer and stored in the desiccator for further use.

5.2. Morphology and distribution of NPs in the DMNs

The morphology of DMNs was visualized using a stereo fluorescence microscope (SZ61-SET, Olympus, Japan). The images of DMNs were further taken by CLSM (FV3000, Olympus, Japan) to determine the distribution of NPs in the DMNs. The excitation and emission wavelength was set at 675 and 694 nm, respectively.

5.3. Skin insertion capability

To evaluate the skin insertion capability, the fabricated DMNs were inserted into the abdominal skin of SD rats using a thumb for 0.5 min. Subsequently, the DMNs were withdrawn to isolate the pierced skin for preparing the histological specimens. Next, the obtained skin was immersed in the 4% paraformaldehyde for H&E staining.

5.4. In vivo dissolution performance

To study the *in vivo* dissolvability of DMNs, the DMNs were inseted into the back skin of mice and taken off at 10, 20 and 30 min. Then, the morphologies of DMNs before and after insertion were observed by an optical microscopy (Nikon, Eclipse Ts2, Japan).

From Fig. S6, it could be seen that the DMNs underwent transition from sharp tips to blunt tips after insertion into the skin, and were completely dissolved within 30 min.

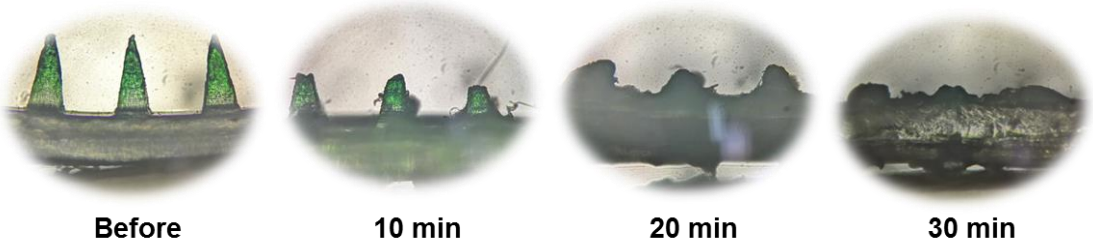

Figure S6 Optical microscopy images of microneedle patches before and after insertion for 10, 20 and 30 min into the back skin of the mice.

5.5. In vitro photothermal conversion efficiency

To test the heating efficacy of the NPs loaded DMNs, the composite DMNs were illuminated with NIR laser (808 nm, 1 W/cm^2) for 5 min. The maximum temperature of composite DMNs was record by an infrared thermal imaging camera (Fluke). The blank DMNs were used as the control.

6. *In vivo* studies

6.1. Experimental animals and xenograft tumor models

Female BALB/c mice of 4-6 weeks were procured from the Laboratory Animal Center of Sun Yat-sen University (Guangzhou, China). All animal experiments were conducted in accordance with the Guide for Care and Use of Laboratory Animals and under the protocols approved by the Institution Animal Care and Use Committee of Sun Yat-sen University (Approval No. SYSU-IACUC-2019-000114).

To establish xenograft tumor models and make it easier for administration, the dorsal hair of mice was removed using electric razor and depilatory paste. Then, 50 μL of 4T1 cells suspended in DMEM culture medium at a density of 2 × 10^6/mice were subcutaneously injected into the back area of mice using a 0.5 mL insulin syringe (Becton Dickinson, NJ, USA). Tumor progression was monitored by calculating the tumor volume (V = 1/2 × Length × Width^2). The length and width of tumors was measured with a vernier caliper. The 4T1 tumor-bearing mice were used when the tumor volume reached 100–150 mm^3.

6.2. Biodistribution and tumor accumulation of HD10 NPs

The mice were randomly divided into two groups and intravenously injected with 100 μL of saline or HD10 NPs (2 mg/kg ICG). The mice were imaged using a small animal imaging system (IVIS® Lumina XRMS Series III, PerkinElmer, USA) at 2, 4, 6, 8, 12 and 24 h after dosing. The excitation and emission wavelength was set at 740

and 790 nm, respectively. At 24 h post-administration, the mice were sacrificed to harvest the major organs (heart, liver, spleen, lung and kidney) and tumors for the *ex vivo* imaging.

Fig. S7 shows the fluorescence images of mice after tail vein injection of saline and HD10 NPs, as well as the distribution of HD10 NPs in the major organs and tumors. No fluorescence signal was detected at any time point in the saline group. The fluorescence intensity of tumor sites in the HD10 NPs group first increased, and then decreased with the extension of time. The maximum fluorescence intensity was achieved after 4 h of administration, which was determined as the time for laser irradiation to provide photothermal therapy. At 24 h post-dosing, bright fluorescence signal could be detected in the tumor tissues, indicating the efficient accumulation of HD10 NPs at the tumor sites. Likewise, obvious fluorescence signal was observed in the liver, lung and kidney, due to the distribution of HD10 NPs in these tissues through systemic circulation.

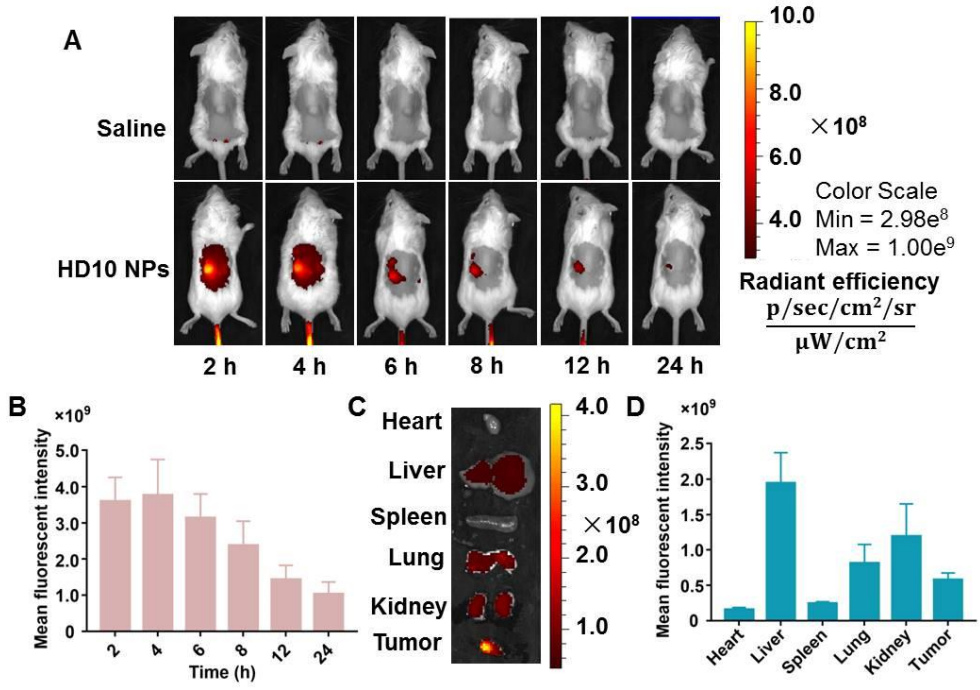

Figure S7 *In vivo* biodistribution and fluorescent imaging of the 4T1 tumor-bearing mice after intravenous injection of saline and HD10 NPs (Data are presented as mean or mean±SD, *n*=4): (A) the fluorescent imaging of mice over 24 h, (B) mean fluorescent intensity at different time intervals, and (C) and (D) the fluorescent

imaging (C) and mean fluorescent intensity (D) of major organs and tumors excised at 24 h post-injection. Among them, (B)–(D) were only designated to the mice with intravenous injection of HD10 NPs.

6.3. In vivo photothermal effect and anti-tumor efficacy

To compare the anti-tumor effect of different administration route and chemo-photothermal combined therapy, the mice were randomly divided into eight groups: (1) no treatment, (2) intravenous injection of HD10 NPs, (3) intratumor injection of HD10 NPs, (4) HD10 NPs loaded DMNs (two patches), (5) intravenous injection of HD10 NPs with LS at 4 h post-administration, (6) intratumor injection of HD10 NPs with LS after administration, (7) HD10 NPs loaded DMNs (two patches) with LS at 0.5 h after the second post-administration, where each patch was retained in the skin for 0.5 h to completely dissolve, and (8) HD10 NP-loaded DMNs (two patches) with LS at 0.5 h. For the intravenous injection group, PTX and ICG was given at the dose of 5 mg/kg and 4 mg/kg, respectively. Each DMNs patch contained 13.8 μg of PTX and 4.1 μg of ICG. To maintain the same PTX dose of local administration, PTX was given at the dose of 27.6 μg/mice, corresponding to the ICG of 22.1 μg/mice in the intratumor injection group.

An infrared thermal imaging camera (TiS75, Fluke, USA) was used to taken the infrared thermal images and record the temperature changes during LS. After treatment, the tumor volume and body weight of each mice were recorded every two days for 20 days. On Day 20 after treatment, the tumor of each mouse was harvested to get tumor weight, and the major organs in each group were collected for H&E staining and pathological investigation.

6.4. Skin recovery of mice treated with DMNs

To evaluate the influence of hypothermia on the normal skin, healthy mice were treated with DMNs plus LS (808 nm, 1 W/cm^2) for 5 min. The untreated mice were used as controls. The photographs of mice were taken at different time intervals. It could be seen from Fig. S8 that the hyperthemia with temperature exceeding 50 ℃

could cause damage to normal tissues, which returned back to normal in about 10 days.

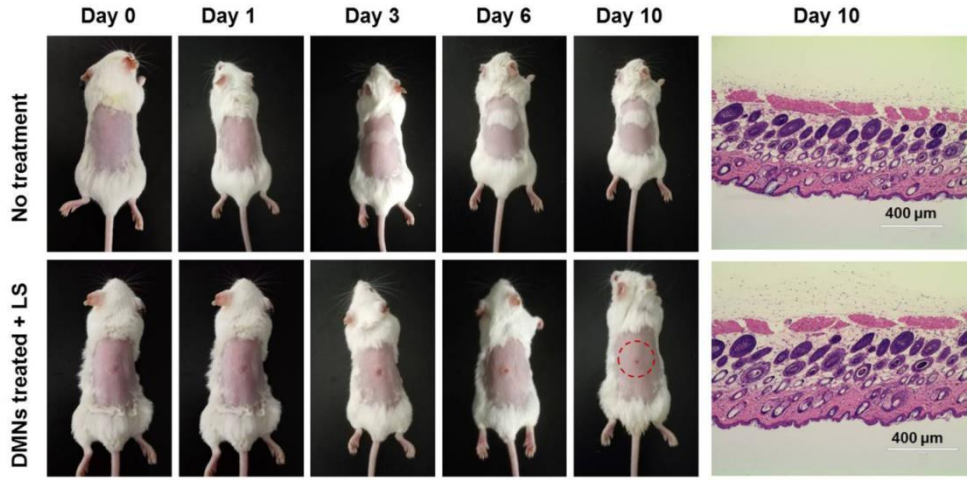

Figure S8 The skin recovery of mice after treatment with DMNs plus LS (808 nm, 1 W/cm^2).

References

1. Zheng M, Yue C, Ma Y, Gong P, Zhao P, Zheng C, et al. Single-step assembly of DOX/ICG loaded lipid–polymer nanoparticles for highly effective chemo-photothermal combination therapy. *ACS Nano* 2013;**7** :2056-67.

2. Zheng C, Zheng M, Gong P, Jia D, Zhang P, Shi B, et al. Indocyanine green-loaded biodegradable tumor targeting nanoprobes for *in vitro* and *in vivo* imaging. *Biomaterials* 2012;33:5603-9.

3. Wang H, Liu C, Gong X, Hu D, Lin R, Sheng Z, et al. *In vivo* photoacoustic molecular imaging of breast carcinoma with folate receptor-targeted indocyanine green nanoprobes. *Nanoscale* 2014;**6**:14270-9.

4. Zhao P, Zheng M, Yue C, Luo Z, Gong P, Gao G, et al. Improving drug accumulation and photothermal efficacy in tumor depending on size of ICG loaded lipid-polymer nanoparticles. *Biomaterials* 2014;35:6037-46.